Published in final edited form as:
*Nucl Med Biol*. 2012 May ; 39(4): 472–483. doi:10.1016/j.nucmedbio.2011.10.020.

# Combined modality radioimmunotherapy: synergistic effect of Paclitaxel and additive effect of Bevacizumab

**B. S. Jang**[a,+], **S. -M. Lee**[a,+], **H. S. Kim**[a], **I. S. Shin**[a], **F. Razjouyan**[b], **S. Wang**[b], **Z. Yao**[a], **I. Pastan**[c], **M. R. Dreher**[b], and **C. H. Paik**[a,*]

[a]Radiopharmaceutical Laboratory, Nuclear Medicine, Radiology and Imaging Sciences, CC, NIH, Bethesda, MD 20892, USA

[b]Center for Interventional Oncology, Radiology and Imaging Sciences, Clinical Center, NCI, NIH, Bethesda, MD 20892, USA

[c]Laboratory of Molecular Biology, NCI, NIH, Bethesda, MD 20892, USA

## Abstract

**Introduction—**This study was undertaken to investigate the effect of Paclitaxel and Bevacizumab on the therapeutic efficacy of $^{90}$Y-labeled B3 mAb, directed against Le$^{y}$ antigen, for the treatment of Le$^{y}$-positive A431 tumors implanted *s.c.* in the right hind flank of nude mice.

**Methods—**When the tumor size reached ~200 mm$^3$, the mice received a single dose of *i.v.* $^{90}$Y-labeled B3 (60 μCi/150 μg or 100 μCi/150 μg B3), *i.p.* Paclitaxel (40 mg/kg), or *i.v.* Bevacizumab (5 mg/kg) for monotherapy. To investigate the effect of combined therapies on survival, the mice were treated with two or three agents in the following combinations: $^{90}$Y-B3 on day 0 and Paclitaxel on day 1; Bevacizumab on −1 day and $^{90}$Y-B3 on day 0; Bevacizumab on −1 day and Paclitaxel on day 1; Bevacizumab, $^{90}$Y-B3, and Paclitaxel each at 1-day intervals. The mice with no treatment were used as a control. The tumor volume at 1,000 mm$^3$ was used as a surrogate endpoint of survival.

**Results—**Compared to control animals, Paclitaxel delayed tumor growth with a significantly longer median survival time ($P < 0.001$) whereas Bevacizumab alone showed a less pronounced effect on a median survival time ($P = 0.18$). $^{90}$Y-B3 increased the median survival time in a dose dependent manner ($P < 0.05$). The combined therapy of Bevacizumab with Paclitaxel produced a trend toward an increase of the median survival time compared to Paclitaxel alone ($P = 0.06$), whereas Bevacizumab combined with $^{90}$Y-B3 showed a statistically insignificant increase in the median survival time compared to $^{90}$Y-B3 alone ($P = 0.25$). The tumor sizes of all animals in these groups reached the surrogate end point of survival by day 35. In contrast, the combined therapy involving $^{90}$Y-B3 with Paclitaxel showed a striking synergistic effect in shrinking tumors and prolonging the survival time ($P < 0.001$); on day 120, 3 of 9 mice (33%) and 6 of 6 mice (100%) were alive without tumor when treated with 60 μCi $^{90}$Y-B3 and 100 μCi $^{90}$Y-B3, respectively. The addition of Bevacizumab treatment one day before the combined therapy of 60 μCi $^{90}$Y-B3 with Paclitaxel did not produce a statistically significant increase in survival when compared to

*Corresponding author: Tel.: +1 301 496 1426, fax: +1 301 402 4548., cpaik@mail.nih.gov (Chang H. Paik, PhD).
+Both authors equally contributed as first authors
Current address: B. S. Jang, VMD, PhD, Radiation Biotechnology Division, Advanced Radiation Technology Institute, Korea Atomic Energy Research Institute, 29 Keumgu-gil, Jeongeup-si, Jeollabuk-do 580-185, South Korea; S.-M. Lee, PhD, Department of Chemical Engineering, Kangwon National University, 1 Kangwondaehak-gil, Chuncheon-si, Gangwon-do 200-701, South Korea.

the $^{90}$Y-B3 with Paclitaxel ($P > 0.10$). Fluorescence microscopy analysis indicated that Paclitaxel increased, whereas Bevacizumab decreased the accumulation and penetration of Alexa Fluor 647-B3 into tumor microenvironment compared to the control ($P < 0.05$).

**Conclusion—**Our findings on the Paclitaxel effect support a hypothesis that the increased tumor accumulation and penetration of $^{90}$Y-B3 as well as the high radio-sensitization of tumor cells by Paclitaxel may be the major factors responsible for the synergistic effect of the combined therapy involving $^{90}$Y-B3 with Paclitaxel.

## 1. Introduction

Monoclonal antibodies (mAbs) labeled with cytotoxic radionuclides have a potential to enhance therapeutic effects of mAbs by systemically delivering a continuous low dose radiation to tumor sites, thereby initiating apoptotic mechanisms through low-dose rate radiation damage to DNA [1, 2]. Two anti-CD20 mAbs armed with Y-90 (Zevalin) and I-131 (Bexxar) have been approved by the FDA for radioimmunotherapy of hematological malignancies [3–5]. Other mAbs with cytotoxic radioisotopes targeting different antigens in hematological malignancies have also shown frequent tumor responses [6, 7]. In contrast to the success shown for radioimmunotherapy of hematological malignancies, the radioimmunotherapy for solid tumors have shown fewer and much diminished tumor responses [8–10]. A variety of impediments have been described in solid tumors to explain the limited targeting of mAb, including vascular, stromal, interstitial and tumor binding-site barriers [11–15]. A high shed antigen concentration in the blood and the interstitial fluid space of tumors also could act as a decoy to antigen-specific tumor targeting of mAbs, thus preventing mAbs from binding to antigens expressed on tumor cells [16]. These barriers often result in limited tumor uptake and heterogeneous distribution of mAbs in solid tumors. The relatively higher radio-resistance of solid tumors also contributes to diminished tumor responses. To overcome the barriers, thereby improving the therapeutic efficacy of immunoconjugates, several approaches have been proposed including the use of physical-mechanical moderators such as hyperthermia [17], and pulsed high intensity focused ultrasound [18] or physiological moderators [15]. In this study, we investigated the effect of physiological moderators, Paclitaxel and Bevacizumab, on the therapeutic efficacy of Y-90 labeled B3 mAb, thereby optimizing a combination therapy regime to cure human tumor implanted in nude mice.

Paclitaxel (Taxol; Bristol-Meyers-Squibb) is a plant alkaloid which promotes the stabilization (polymerization) of microtubules leading to mitotic arrest at a radiosensitive G2/M phase that disrupts the cell division process and causes cell death [19–21]. It also induces bcl-2 phosphorylation, and subsequent caspase-3-dependent and caspase-3-independent apoptosis [22, 23]. The role of Paclitaxel is well established in the treatment of advanced breast cancer, and its use was recommended by USA and European Union (EU) guidelines and a recent consensus manuscript [24–26]. A number of preclinical investigations have reported that Paclitaxel increased the therapeutic efficacy of Y-90 labeled mAb. A higher number of complete response (CR) were achieved when the animals were treated with $^{90}$Y-antibody at a dose below a maximum tolerated dose (MTD) in combination with Paclitaxel [27–31]. Miers, et al reported that Paclitaxel given after $^{111}$In-labeled mAbs increased tumor-cumulated activity by 30% in epithelial cancers [32]. Paclitaxel has also been shown to decrease tumor interstitial fluid pressure (IFP), which may aid the delivery of convection-dominated macromolecules such as antibodies [33]. The Paclitaxel effects on radiosensitization of tumor cells and increased delivery of radiolabeled mAb to tumors make a combined radioimmunotherapy with Paclitaxel an attractive approach.

Bevacizumab (Avastin; Genentech, California) is a humanized monoclonal antibody directed against vascular endothelial growth factor (VEGF). VEGF stimulates the growth of new blood vessels [34–36]. VEGFs and their receptors are key molecules in the regulation of vessel growth [37–39]. The specific binding of Bevacizumab to VEGF prevents VEGF from interacting with receptors on vascular endothelial cells, thereby inhibiting its pro-angiogenic effects [40, 41]. As a result, Bevacizumab decreases micro-vascular density by pruning immature blood vessels and reduces vascular permeability in tumors [42]. Direct correlations were also shown between density of microvessels, metastases and survival of patients [37, 38]. Bevacizumab is currently approved for the treatment of metastatic colorectal cancer, non-small-cell lung cancer, and renal cell cancer [43, 44]. It is also approved in the United States for the treatment of recurrent glioblastoma multiforme [43]. Recently, Jain et al. showed that antiangiogenic drugs such as Bevacizumab could induce a functional normalization of the tumor vasculature over a transient span of time (normalization time window) during which time it increases tumor oxygenation and the tumor concentration of coadministered drugs, thereby potentiating the activity of coadministered chemo or external radiotherapies [45]. However, chronic angiogenesis inhibition is known to destroy or block the function of tumor-associated vessels to deprive the tumor of oxygen and nutrients and also reduces tumor uptake of coadministered chemotherapeutics [46]. Ansiaux, et al. subsequently demonstrated that the VEGF and basic fibroblast growth factor inhibitor, thalidomide was able to increase tumor oxygenation by modifying tumor perfusion and interstitial pressure [47]. This finding was supported by Ruud, et al. showing that angiogenesis inhibitors Anginex and Bevacizumab transiently increased overall tumor oxygenation via vessel normalization [48]. They also showed that this increase in oxygenation enhanced the effect of radiation therapy *in vivo* especially when radiation was applied at the peak of tumor oxygenation during therapy. Furthermore, they found the normalization window induced by Bevacizumab within the first few days of treatment, similar to that found for thalidomide and VEGFR2 inhibitor [47]. After those first few days of the antiangiogenic treatment, there was a progressive decrease in tumor oxygenation. Salaun, et al. reported that pretreatment with Bevacizumab improved radioimmunotherapy efficacy, with similar toxicity as compared to radioimmunotherapy alone in a mouse model of medullary thyroid carcinoma [49]. Bevacizumab also demonstrated considerable efficacy in combination with taxane therapy in the first-line treatment of human epidermal growth factor receptor-2 (HER2)-negative metastatic breast cancer in three phase III trials [50]. These studies indicate that the addition of antiangiogenic drugs in combination with chemo- and radio-therapy in a proper sequence, time interval, and dose may help enhancing the therapeutic efficacy; however, the influence of antiangiogenic drugs on the delivery of radioimmunotherapy remains unknown.

B3 is a murine IgG1κ mAb which reacts with a carbohydrate epitope found on $Le^y$ and polyfucosylated $Le^x$ antigens. This epitope is abundantly and uniformly expressed by most carcinomas of stomach, colon, breast, lung, bladder, and ovary [51]. A preclinical biodistribution study of $^{111}In/^{90}Y$-radiolabeled B3 antibody has shown good tumor localization in the antigen-positive A431 tumor xenografted in nude mice [52, 53]. In a Phase 1 trial with $^{111}In$- and $^{90}Y$-B3, definite tumor imaging was observed in 20 of 26 patients, but no antitumor effect was observed, presumably because of the insufficient dose delivered to tumors before dose limiting toxicity was reached [10]. For the treatment of radio-resistant solid tumors with a radioimmunotherapy, it is a critical factor to increase a radiation dose delivered to tumors and also make tumor cells more radiosensitive to a continuous low-dose radiation. This led us to undertake our preclinical study to investigate if combined modality radioimmunotherapies involving $^{90}Y$-B3 mAb in combination with Paclitaxel and Bevacizumab could produce a synergistic or an additive effect at a dose which is not sufficient to produce a positive tumor response when given individually. We also investigated the effect of Paclitaxel and Bevacizumab on blood vessel density, vessel

size, and the tumor microdistribution of fluorophore labeled B3 (Alexa Fluor 647-B3) by fluorescence microscopic analysis. In this study, we used a mouse model of human A431 tumor which overexpress $Le^y$ antigen.

## 2. Experimental Procedure

### 2.1. Radiolabeling of B3 with $^{90}Y$

B3 conjugated with 2-(*p*-SCN-Bz)-6-methyl-DTPA (MX) was radiolabeled with $^{90}Y$ using a method reported previously [53]. Briefly, 10 mCi of $^{90}YCl_3$ (PerkinElmer, Boston, MA; 10 mCi/40 μl of 0.05 M HC1) was adjusted to pH 4.2 with a 200 μl of buffer solution containing 0.30 M sodium acetate and 0.040 M sodium ascorbate in a polypropylene vial. Typically, 60 μl of antibody solution (10.8 mg/ml, pH 7) was added and allowed to react at pH 4.2 at room temperature for 15 min. To this reaction mixture, 30 μl of 1 mM DTPA was added and the solution was incubated at room temperature for 5 min to complex any free $^{90}Y$ ions with DTPA. The radiolabeling yield was determined by instant thin layer chromatography with silica gel impregnated on glass fiber (ITLC; Gelman Sciences, Ann Arbor, MI) developed with 10% ammonium acetate in water:methanol (1:1). The radioactivity peak areas were integrated with a Bioscan radiochromatogram scanner (Bioscan Inc, Washington, DC). On ITLC, the radiolabeled antibody remains at the origin of application and $^{90}Y$-DTPA moves with the solvent front. Radiolabeled antibody preparations were purified with a PD-10 size exclusion column (GE Healthcare Bio-Sciences AB, Uppsala, Sweden) with PBS as the elution buffer. The radiochemical purity was assessed by HPLC (Gilson, Middleton, WI) equipped with a size exclusion TSK gel $G3000SW_{XL}$ column (7.8 × 300 mm, 5 μm, TOSOH Bioscience, Japan; 0.067 M sodium phosphate/0.15 M sodium chloride, pH 6.8; 1.0 ml/min), a UV monitor and an on-line flow radioactivity detector (Bioscan Inc., Washington, DC). The specific activity of $^{90}Y$-B3 was ~10 μCi/μg B3. The radiochemical purity and immunoreactivity of the purified $^{90}Y$-B3 was >98% and 70%, respectively.

### 2.2. Conjugation of Alexa Fluor 647 to B3

A fresh solution (1.99 mM) of succinimidyl ester of Alexa Fluor 647 (Invitrogen) in anhydrous DMSO was prepared. Forty μl (79.6 nmol) of this solution was immediately added to 760 μl of B3 (4.0 mg, 26.6 nmol) dissolved in 0.25 M of sodium bicarbonate solution, pH 8.4. The solution was mixed thoroughly and let stand for 1 hr at room temperature. The reaction mixture was analyzed by size-exclusion HPLC (Gilson, Middleton, WI) connected with a UV/Visible detector set at a wavelength maximum of 650 nm. The conjugation efficiency was then determined by comparing the peak intensity of Alexa Fluor 647-conjugated B3 and that of free Alexa Fluor 647 on the HPLC profiles. This reaction resulted in Alexa Fluor 647-conjugatd B3 with ~2 Alexa Fluor 647 molecules per B3. The product, Alexa Fluor 647-B3 was purified with a size exclusion PD-10 column (GE Healthcare Bio-Sciences AB, Uppsala, Sweden) with PBS as the elution buffer. An aliquot (100 μg/100 μl PBS, pH 7.2) of the purified Alexa Fluor 647-B3 and unconjugated B3 were labeled with $^{125}I$ (500 μCi) with 4-[$^{125}I$]iodobenzoate [54] at a specific activity of ~1.0 μCi/μg. The iodinated B3 preparations were purified with a PD-10 column as described above. The immunoreactivity of $^{125}I$ labeled Alexa Fluor 647-B3 was determined to be >68% using a cell-binding assay reported previously [54].

### 2.3. Cell Culture

A431, a human epidermoid carcinoma cell line that expresses the $Le^y$ antigen recognized by B3, was grown in RPMI 1640 supplemented with 10% FCS, 2 mM L-glutamine, penicillin (100 IU/ml), and streptomycin (100 μg/ml) at 37°C in a humidified atmosphere with 5% $CO_2$. Cells were harvested with EDTA-trypsin, washed with PBS and resuspended in PBS

with 1% BSA for immunoreactivity determination or resuspended in PBS to make a mouse model of A431 human tumor.

### 2.3. Tumor Model

Animal experiments were performed under an NIH Animal Care and Use Committee approved protocol. Tumor xenografts were established by *s.c.* inoculation of $3 \times 10^6$ A431 cells in 0.1 ml PBS into the right flank of athymic mice (5–6 weeks, 18–20 g; NCI-DCT, Frederick, MD). Tumor dimensions were measured using a caliper. Tumor size ($mm^3$) was calculated by the following formula: $(a) \times (b)^2 \times 0.4$, where a is tumor length (max) and b is tumor width (min) in millimeters.

### 2.4. Therapeutic studies

Groups of nude mice (n = 4–9 mice/group) were inoculated *s.c.* with A431 tumor cells expressing the $Le^y$ antigen on the right hind flank. When the tumor size was approximately 200 $mm^3$, the mice received a single dose of *i.v.* $^{90}$Y-labeled B3 (60 μCi/150 μg or 100 μCi/150 μg B3), *i.p.* Paclitaxel (40 mg/kg), or *i.v.* Bevacizumab (5 mg/kg) for a monotherapy. For a combined radioimmunotherapy with Paclitaxel or Bevacizumab, the mice received $^{90}$Y-B3 (60 μCi/150 μg $^{90}$Y-B3 or 100 μCi/150 μg) followed by Paclitaxel (40 mg/kg) or Bevacizumab (5 mg/kg) followed by $^{90}$Y-B3 (60 μCi/150 μg $^{90}$Y-B3) at 1-day interval. For a combined therapy of Paclitaxel with Bevacizumab, the mice first received Bevacizumab followed by Paclitaxel treatment 48 hr later. For a combined therapy with three agents, the mice were treated with Bevacizumab, $^{90}$Y -B3 (60 μCi/150 μg) and Paclitaxel each at 1 day intervals. The mice with no treatment were used as a control. The treatment time line is shown in Fig. 1. The tumor volume and the body weight were measured daily for the first 7 days and thereafter, two or three times a week. Mice were euthanized when the tumor size was 2 cm in diameter, or the body weight was reduced by >15% of the initial value. To estimate survival time, the tumor volume was plotted over time for each mouse and the day at which tumor volume passed 1,000 $mm^3$ was used as a surrogate endpoint of survival. In some cases, to estimate survival times objectively, a polynomial trendline of Microsoft Office Excel 2007 was used for fitting the tumor growth curves. The time required for the tumor growth curves or the trendline curves to reach the tumor volume at 1,000 $mm^3$ was taken as the survival time. Survival is displayed as a Kaplan-Meier plot to compare the therapeutic efficacy of each treatment regime. The Kaplan-Meir plot was performed using GraphPad Prism 5 (GraphPad Software, La Jolla, CA). To construct mean tumor growth curves, the tumor volume of each mouse was measured at each time point and the day at which tumor volume passed 1,000 $mm^3$ was used as a surrogate endpoint. If mice reached this surrogate endpoint, their tumor volume at 1,000 $mm^3$ was used from that point forward and contributed to the calculation of the mean tumor volume. The mean tumor volume calculated at each time point was plotted over time to construct the mean tumor growth curve.

### 2.5. Ex vivo fluorescence microscopy studies

Groups of nude mice (n = 4~5 mice/group) were inoculated *s.c.* with A431 tumor cells expressing the $Le^y$ antigen on the right hind flank. When the tumor size reached ~200 $mm^3$, the tumor-bearing mice were injected with *i.v.* Alexa Fluor 647-conjugated B3 (150 μg in 0.2 ml of PBS) alone on day 0, *i.v.* Alexa Fluor 647-B3 on day 0 followed by *i.p.* Paclitaxel (40 mg/kg in 0.2 ml of normal saline) on day 1, or *i.v.* Bevacizumab (5 mg/kg in 0.2 ml of PBS) on day 0 followed by *i.v.* Alexa Fluor 647-B3 on day 1 to investigate the effect of Paclitaxel and Bevacizumab on the tumor microdisribution of Alexa Fluor 647-B3. Two days after the injection of Alexa Fluor 647-B3, the mice received a lateral tail vein injection of rhodamine-lectin (RCA, 1 mg in 0.2 ml of PBS) to delineate the blood vessels and 5 min after the lectin injection, the mice were euthanized by $CO_2$ inhalation and exsanguinated by

cardiac puncture before dissection. Tumors were harvested with intact skin and flash-frozen using liquid nitrogen for subsequent sectioning and staining. Tumors were sectioned using a Leica CM1850 cryostat at 8 μm thickness in 3 different regions to obtain representative sections throughout the tumor. Tumor sections were fixed with formalin for 20 min and mounted with Prolong Gold antifade reagent with DAPI (Invitrogen, Carlsbad, CA). Imaging was performed with a 10X objective (pixel size = 0.64 μm, binning 2×2) using an epi-fluorescent microscope (Zeiss, Axio Imager.M1, Thornwood, NY) equipped with a motorized scanning stage and mosaic stitching software (Axiovision, Zeiss). Three independent channels were obtained: DAPI for nuclei (shown in blue), Rhodamine for blood vessels (shown in red), and Cy5 for Alexa Fluor 647-B3 antibody (constant exposure time of 40 ms, shown in green). A tumor that did not contain B3 antibody was imaged with identical parameters to obtain background signal intensity. Image analysis was performed with a custom-designed MATLAB script (MathWorks, Natick, MA). Individual image channels were exported from Axiovision as 16-bit grayscale tiff images to Photoshop where a tumor region was isolated to create a tumor mask. The tumor mask, blood vessel image and B3 antibody image were loaded into MATLAB and a tumor blood vessel mask and distance map were created [55]. Overall B3 antibody intensity and penetration from the tumor edge and blood vessel surface were calculated with a background intensity subtraction. In addition, vascular parameters and architecture such as micro-vasculature density (MVD), blood vessel size, and median distance from a tumor pixel to the nearest vascular surface were measured. Values were grouped together from the 3 tumor regions to represent a tumor. Each tumor was treated as an independent sample (n= 4–5, one tumor was removed due to excessive necrosis limiting analysis).

### 2.6. Statistical analysis

All statistical analyses for the therapeutic studies were performed using Student's t test for unpaired data between two groups. All tests were two-sided, and a probability value (P) of less than 0.05 was considered significant. Fluorescence microscopy data are reported as mean ± standard error of the mean (SEM) and analyzed with a one-way ANOVA followed by a Newman-Keuls post-hoc test between multiple groups. P-values less than 0.05 were considered statistically significant and all statistical tests were two-sided.

## 3. Results

### 3.1. Therapeutic Studies

The tumors in the control group grew rapidly with a median survival time of 4 days (Table 1 and Fig. 2). The Bevacizumab (5 mg/kg) treatment provided a statistically insignificant delay in tumor growth with a median survival time of 6 days ($P > 0.05$ compared to the control). The Paclitaxel (40 mg/kg) treatment initially stabilized the tumor growth for 5 days and thereafter, the tumors started re-growing with a statistically significant delay of a median survival time to 11 days compared to the control ($P < 0.001$). The $^{90}$Y-B3 treatment also slowed the tumor growth rate with a median survival time in a dose dependent manner; 14 days for 60 μCi/150 μg B3 and 23 days for 100 μCi/150 μg B3 ($P < 0.05$ compared to the control). The combined therapy involving Bevacizumab followed by Paclitaxel treatment showed a trend toward a moderate additive effect in prolonging the median survival time to 16 days compared to the median survival time of 11 days for the Paclitaxel alone group ($P = 0.06$). The addition of Bevacizumab one day before $^{90}$Y-B3 treatment also produced an additive effect on survival by 2 days compared to that of $^{90}$Y-B3 alone ($P = 0.25$). However, this additive effect was statistically not significant. The tumor volumes of all animals in the above study groups reached the surrogate end point (1000 mm$^3$) by day 35. In contrast, the combined therapy involving $^{90}$Y-B3 with Paclitaxel showed a striking synergistic effect in shrinking tumor and prolonging the survival time ($P < 0.001$ compared to each agent). On

day 120, 3 of 9 mice (33%) and 6 of 6 mice (100%) were alive with no tumor when treated with a combined therapy involving 60 μCi B3 and Paclitaxel, and 100 μCi B3 and Paclitaxel, respectively. The addition of Bevacizumab treatment to the combined therapy of 60 μCi B3 and Paclitaxel provided some additive effect in survival with 3 of 6 (50%) alive with no tumor as compared to 3 of 9 (33%) alive for the combined therapy of 60 μCi B3 and Paclitaxel (Table 1 and Fig. 2), but this difference in survival time between these two groups is statistically insignificant ($P > 0.05$). The mean tumor growth curves (Fig. 3) show the effect of different treatment regimes on the growth delays.

### 3.2. Microvascular analysis

We investigated the effect of Paclitaxel and Bevacizumab on the tumor micro-vascular density (MVD), blood vessel size, and median distance from a tumor pixel to the nearest vascular surface (Fig. 5). The vasculature and cell nuclei were stained with rhodamine-lectin and DAPI, respectively. The fluorescence microscopic determination revealed that Paclitaxel (40 mg/kg) treatment did not significantly change the MVD (67.4 vs 70.3 vessels/$mm^2$ for the control, $P > 0.05$) (Fig. 5A), median blood vessel area (92.7 vs 100.1 $\mu m^2$ for the control) (Fig. 5B), and the median distance to the nearest vascular surface, an indicator of vascular architecture (78.8 vs 69.3 μm for the control, $P > 0.05$) (Fig. 5C) compared to the control one day after the treatment. Comparatively, the treatment with Bevacizumab decreased the MVD (53.4 vessels/$mm^2$) by 24% and increased the median distance (95.1 μm) from a tumor pixel to the nearest vascular surface by 37% compared to the control, although statistically not significant ($P > 0.05$). Bevacizumab did not change the median blood vessel size (92.22 $\mu m^2$).

### 3.3. Antibody accumulation and penetration

Antibody accumulation was determined by analyzing fluorescence intensity in tumor sections. The analysis qualitatively suggests that B3 antibody (green) accumulation and penetration was improved with Paclitaxel treatment and reduced with Bevacizumab treatment (Fig. 4). The image analysis demonstrated that Paclitaxel treatment significantly improved B3 antibody delivery to the tumor by 45% (2570 vs 1775 arbitrary fluorescence units for the control, $P < 0.05$) (Fig. 5D). The B3 penetration was significantly improved following treatment with Paclitaxel both from the tumor surface and from the blood vessel surface ($P < 0.05$) (Fig. 6). The Paclitaxel treatment also appeared to impact the integrity of the tumor tissue with a muddled cell nuclei appearance (Fig. 4). Comparatively, Bevacizumab had a profound effect on B3 antibody delivery, significantly reducing the accumulation by 96% (73 vs 1775 for the control, $P < 0.05$) (Fig. 5D). In addition, Bevacizumab significantly reduced the penetration of B3 antibody ($P < 0.05$) (Fig. 6).

## 4. Discussion

The purpose of this study was to investigate combined modal radioimmunotherapy regimen involving Paclitaxel, Bevacizumab, and $^{90}$Y-B3, each of which acts on tumor cells and the tumor microenvironment by different mechanisms, thereby finding an effective regimen to cure A431 tumors implanted in nude mice. For combined modality radioimmunotherapies, the animals were treated with $^{90}$Y-B3 a day after Bevacizumab, and/or a day before Paclitaxel. We used these treatment sequences because these treatment sequences were reported to produce the best therapeutic effects [27, 49]. To investigate if the combined therapy increased the therapeutic efficacy, we used each drug at a dose which is ineffective in curing tumors and also does not cause serious side effects to the animals (defined by body weight loss). The dose (60 and 100 μCi) of $^{90}$Y-B3 used in this study are much lower than the maximum tolerated dose (200~300 μCi) of $^{90}$Y-B3. We used a single Bevacizumab dose (5 mg/kg) which is lower than a total daily dose of 5 mg/kg, 5 days a week, i.p. investigated

by Bozec, et al [56] and a dose of 5 mg/kg, twice weekly for 4 weeks, i.p. by Salaun, et al [49]. They reported that Bevacizumab alone induced no cytopenia and no significant weight loss. The Paclitaxel dose (40 mg/kg) used in this study is equivalent to a human dose of 123 mg/m$^2$, within the doses usually used for treatment of women with metastatic breast cancer (100–250 mg/m$^2$) [32]. Other groups reported up to 50 mg/kg [57] and 75 mg/kg [58] of Paclitaxel to investigate its antitumor activity in mice without observing a dose limiting adverse effect.

The treatment with Paclitaxel (40 mg/kg) alone and Bevacizumab (5 mg/kg) alone prolonged the median survival time by 7 days ($P < 0.05$) and by 2 days ($P > 0.05$), respectively compared to the control. The treatment with $^{90}$Y-B3 (60 μCi/150 μg B3 or 100 μCi/150 μg B3) alone also increased the median survival time in a dose dependent manner ($P < 0.05$). The addition of Bevacizumab to Paclitaxel treatment produced a trend ($P = 0.06$) toward the prolongation of the median survival time by 5 days compared to Paclitaxel treatment alone. This additive effect is consistent with those reported previously [46, 49]. The addition of Bevacizumab to $^{90}$Y-B3 (60 μCi/150 μg B3) increased the median survival time by 2 days compared to $^{90}$Y-B3 alone, but the difference was statistically insignificant ($P = 0.25$). Since Paclitaxel is a small molecule it is most likely more perfusion-limited than the permeability-limited B3 antibody such that a reduced vascular permeability following Bevacizumab therapy [59] may more adversely affect B3 antibody delivery than Paclitaxel delivery [60]. This difference in delivery may explain some difference shown in the therapeutic efficacy. However, it should be also noted that the use of Bevacizumab for the treatment of metastatic HER2-negative breast cancer in combination with Paclitaxel was debated by a FDA advisory committee and was not approved on June 29, 2011 because the ability to slow the tumor growth determined by medical imaging studies has not been translated into meaningful benefit in overall survival among breast cancer patients. In our study, the tumor volumes of all animals treated with each agent alone or the above combination regimens reached the surrogate endpoint of survival (1000 mm$^3$) by day 35.

In contrast, the combined therapy involving $^{90}$Y-B3 treatment followed by Paclitaxel treatment produced a remarkable synergistic effect on tumor shrinkage and an increase in median survival time; 3 of 9 mice (33%) and 6 of 6 mice (100%) were alive with no tumor ($P < 0.001$) on day 120 when treated with a combined therapy involving 60 μCi $^{90}$Y-B3 or 100 μCi $^{90}$Y-B3 and Paclitaxel, respectively (Table 1 and Fig. 1). The synergistic effects observed in this study are consistent with the results reported by others [27–31]. The addition of Bevacizumab treatment to the combined therapy of 60 μCi $^{90}$Y-B3 and Paclitaxel provided an additive effect in survival with 3 of 6 (50%) alive with no tumor compared to a survival rate of 33% for the combined therapy of 60 μCi $^{90}$Y-B3 and Paclitaxel (Table 1 and Fig. 1). However, this Bevacizumab effect was statistically insignificant ($P > 0.05$). In this study, increasing the dose from 60 μCi to 100 μCi $^{90}$Y-B3 combined with Paclitaxel treatment resulted in survival with no tumor on day 120 in 6 of 6 mice. In addition, there was no animal with loss of body weight by >15% of the initial weight during a 120-day period which indirectly provided an additional evidence for a lack of any severe side effects.

Since Paclitaxel can act on tumor cells as well as the endothelial cells of rapidly growing angiogenic blood vessels, and Bevacizumab is an anti-angiogenic agent, we investigated the effect of Paclitaxel and Bevacizumab on the tumor blood vessels as well as their effects on the microdistribution of Alexa Fluor 647-B3 in tumors by fluorescence microscopy. Compared to control tumors, the fluorescence microscopy analysis showed that the Paclitaxel (40 mg/kg) treatment increased the total accumulation of Alexa Fluor 647-B3 by 45% in the tumor ($P < 0.05$) and facilitated more uniform distribution of Alexa Fluor 647-B3 in the tumor when the analysis was performed one day after Paclitaxel treatment ($P <$

0.05). However, at this time, the Paclitaxel treatment did not cause any statistically significant changes in the MVD and the median blood vessel area. This finding together with the fact that the Paclitaxel treatment impacted the integrity of the tumor tissue with a muddled cell nuclei appearance suggests that the increased accumulation and penetration of Alexa Fluor 647-B3 into tumors by Paclitaxel treatment was the result of the decreased interstitial fluid pressure due to the loss of integrity of the tumor tissue [33, 61]. Although the mechanism of the synergy by the combined therapy is not clearly understood at the present time, our finding supports a hypothesis that the increased accumulation of $^{90}$Y-B3 in tumor and the high radio-sensitization of tumor cells by Paclitaxel are two important factors responsible for the striking synergistic effect when $^{90}$Y-B3 is combined with Paclitaxel. Likewise, we did not investigate the effect of Bevacizumab on the microdistribution of Paclitaxel in tumors or the effect of Paclitaxel on the microdistribution of Bevacizumab. However, our therapeutic studies showed that the addition of Bevacizumab produced a more pronounced trend toward an additive effect in prolongation of the survival time (16 vs 11 days for Paclitaxel alone) when it was combined with Paclitaxel treatment than when it was combined with $^{90}$Y-B3 treatment (16 vs 14 days for $^{90}$Y-B3 alone). This finding appears to indicate that within the time window we investigated, Bevacizumab might have improved the delivery of a small molecule, Paclitaxel to tumor microenvironment as proposed by Jain, et al [45] whereas it decreased the delivery of a large molecule, $^{90}$Y-B3 to tumor as shown in this fluorescence microscopy study. There are three possible hypotheses to explain this additive effect. 1) The antiangiogenic agent Bevacizumab improves tumor uptake of B3. However, this hypothesis is ruled out because our microscopy analysis showed that Bevacizumab decreased the delivery of B3 to tumor microenvironment. 2) Bevacizumab normalizes vascularization, increases tumor perfusion of the small molecular drug Paclitaxel, reduces hypoxia, and increases radiosensitivity of tumor cells [62]. This hypothesis is supported by our finding that Bevacizumab produced a trend toward an additive effect on the survival time when added to Paclitaxel. 3) VEGF is a cytokine, which optimizes the survival of endothelial cells under stress. By inhibiting these endothelial survival pathways, the antiangiogenic agent could sensitize endothelial cells to radiation delivered by radioimmunotherapy, increase death of endothelial cells, and, in turn, reduce tumor growth [63]. Although the precise mechanism of the synergistic effect and the additive effect shown in this study is not yet clearly understood at the present time, the results of our therapeutic studies indicate that the treatment dose, treatment sequence, and time interval were well balanced to cure 6 of 6 mice with tumors at an initial mean tumor size of 200 mm$^3$. This finding implies that it may be possible to cure solid tumors in patients by a combined modality radioimmunotherapy if one could increase the accumulation and penetration of Paclitaxel and $^{90}$Y-mAb into tumor microenvironment, thereby sensitizing more tumor cells to the radiation from $^{90}$Y-mAb. Ytttrium-90 is a high-energy pure beta-emitter with a physical $t_{1/2}$ of 64 h and $E_{max}$ of 2.28 MeV with an average decay energy of 0.94 MeV. The average penetration depth of $^{90}$Y beta emission in human tissue is 2.4 mm, and its tissue maximum range is 1.1 cm [64]. The physical half-life of $^{90}$Y matches well with the biological half-life of mAb, and its maximum radiation penetration distance in tissue of about 1 cm makes it possible to kill several hundred cells by crossfire effect even if heterogeneous antigen expression, tumor architecture, or other factors impede targeting of every cell by the labeled mAb [65]. In this regard, it appears that a homogeneous microdistribution of Paclitaxel is a more important factor than that of $^{90}$Y-B3 for an effective combined radioimmunotherapy with Paclitaxel. This study also suggests that it would be worthwhile to investigate other agents to enhance delivery of Paclitaxel and $^{90}$Y-B3 to tumor such as a tumor-penetrating peptide, CRGDKGPDC (iRGD) recently reported by Ruouslahti, et al. [66]. The influence of tumor microdistribution on combined tumor radioimmunotherapy regimens represents a promising area for further investigation and optimization to improve radioimmunotherapy for solid tumors in the clinic.

## 5. Conclusion

The synergistic effect of Paclitaxel and the additive effect of Bevacizumab to the radioimmunotherapy shown in these studies are very encouraging, considering that the $^{90}$Y-B3 dose used in these studies was much lower than the maximum tolerated dose (200~300 μCi) of $^{90}$Y-B3, as was the dose of Paclitaxel (40 mg/kg) and Bevacizumab (5 mg/kg), suggesting that the combination therapy is clinically achievable. Tumor microdistribution may play an important role in solid tumor radioimmunotherapy.

## Acknowledgments

This research was supported by the intramural research program of Clinical Center, NIH and the Center for Interventional Oncology, NIH. We thank Dr. Bradford Wood for his useful discussion and support of this study. We also thank Dr. Insook Kim for her critical review and editorial assistance of this manuscript.

## References

1. Macklis RM, Beresford BA, Palayoor S, Sweeney S, Humm JL. Cell cycle alterations, apoptosis, and response to low-dose-rate radioimmunotherapy in lymphoma cells. Int J Radiat Oncol Biol Phys. 1993; 27:643–50. [PubMed: 8226159]
2. Kroger LA, DeNardo GL, Gumerlock PH, Xiong CY, Winthrop MD, Shi XB, et al. Apoptosis-related gene and protein expression in human lymphoma xenografts (Raji) after low dose rate radiation using 67Cu-2IT-BAT-Lym-1 radioimmunotherapy. Cancer Biother Radiopharm. 2001; 16:213–25. [PubMed: 11471486]
3. Kaminski MS, Zelenetz AD, Press OW, Saleh M, Leonard J, Fehrenbacher L, et al. Pivotal study of iodine I 131 Tositumomab for chemotherapy-refractory low-grade or transformed low-grade B-cell non-Hodgkin's lymphomas. J Clin Oncol. 2001; 19:3918–28. [PubMed: 11579112]
4. Witzig TE, Gordon LI, Cabanillas F, Czuczman MS, Emmanouilides C, Joyce R, et al. Randomized controlled trial of yttrium-90-labeled ibritumomab tiuxetan radioimmunotherapy versus rituximab immunotherapy for patients with relapsed or refractory low-grade, follicular, or transformed B-cell non-Hodgkin's lymphoma. J Clin Oncol. 2002; 20:2453–63. [PubMed: 12011122]
5. Weigert O, Illidge T, Hiddemann W, Dreyling M. Recommendations for the use of Yttrium-90 ibritumomab tiuxetan in malignant lymphoma. Cancer. 2006; 107:686–95. [PubMed: 16826593]
6. Waldmann TA, White JD, Carrasquillo JA, Reynolds JC, Paik CH, Gansow OA, et al. Radioimmunotherapy of Interleukin-2r-Alpha-Expressing Adult T-Cell Leukemia with Yttrium-90-Labeled Anti-Tac. Blood. 1995; 86:4063–75. [PubMed: 7492762]
7. DeNardo GL, Sysko VV, DeNardo SJ. Cure of incurable lymphoma. Int J Radiat Oncol Biol Phys. 2006; 66:S46–56. [PubMed: 16979440]
8. Mulligan T, Carrasquillo JA, Chung Y, Milenic DE, Schlom J, Feuerstein I, et al. Phase I study of intravenous Lu-177-labeled CC49 murine monoclonal antibody in patients with advanced adenocarcinoma. Clin Cancer Res. 1995; 1:1447–54. [PubMed: 9815943]
9. Yu B, Carrasquillo J, Milenic D, Chung Y, Perentesis P, Feuerestein I, et al. Phase I trial of iodine 131-labeled COL-1 in patients with gastrointestinal malignancies: Influence of serum carcinoembryonic antigen and tumor bulk on pharmacokinetics. J Clin Oncol. 1996; 14:1798–809. [PubMed: 8656248]
10. Pai-Scherf LH, Carrasquillo JA, Paik C, Gansow O, Whatley M, Pearson D, et al. Imaging and phase I study of 111In- and 90Y-labeled anti-LewisY monoclonal antibody B3. Clin Cancer Res. 2000; 6:1720–30. [PubMed: 10815890]
11. Boucher Y, Baxter LT, Jain RK. Interstitial Pressure-Gradients in Tissue-Isolated and Subcutaneous Tumors - Implications for Therapy. Cancer Res. 1990; 50:4478–84. [PubMed: 2369726]
12. Fujimori K, Covell DG, Fletcher JE, Weinstein JN. A modeling analysis of monoclonal antibody percolation through tumors: a binding-site barrier. J Nucl Med. 1990; 31:1191–8. [PubMed: 2362198]

13. Saga T, Neumann RD, Heya T, Sato J, Kinuya S, Le N, et al. Targeting cancer micrometastases with monoclonal antibodies: a binding-site barrier. Proc Natl Acad Sci U S A. 1995; 92:8999–9003. [PubMed: 7568060]
14. Christiansen J, Rajasekaran AK. Biological impediments to monoclonal antibody-based cancer immunotherapy. Mol Cancer Ther. 2004; 3:1493–501. [PubMed: 15542788]
15. Jain M, Venkatraman G, Batra SK. Optimization of Radioimmunotherapy of solid tumors: Biological impediments and their modulation. Clin Cancer Res. 2007; 13:1374–82. [PubMed: 17309914]
16. Zhang Y, Xiang L, Hassan R, Pastan I. Immunotoxin and Taxol synergy results from a decrease in shed mesothelin levels in the extracellular space of tumors. Proc Natl Acad Sci U S A. 2007; 104:17099–104. [PubMed: 17940013]
17. Hauck ML, Zalutsky MR. Enhanced tumour uptake of radiolabelled antibodies by hyperthermia. Part II: Application of the thermal equivalency equation. Int J Hyperthermia. 2005; 21:13–27. [PubMed: 15764348]
18. Khaibullina A, Jang BS, Sun H, Le N, Yu S, Frenkel V, et al. Pulsed high-intensity focused ultrasound enhances uptake of radiolabeled monoclonal antibody to human epidermoid tumor in nude mice. J Nucl Med. 2008; 49:295–302. [PubMed: 18199622]
19. De Brabander M, Geuens G, Nuydens R, Willebrords R, De Mey J. Taxol induces the assembly of free microtubules in living cells and blocks the organizing capacity of the centrosomes and kinetochores. Proc Natl Acad Sci U S A. 1981; 78:5608–612. [PubMed: 6117858]
20. Manfredi JJ, Horwitz SB. Taxol: an antimitotic agent with a new mechanism of action. Pharmacol Ther. 1984; 25:83–125. [PubMed: 6149569]
21. Moos PJ, Fitzpatrick FA. Taxanes propagate apoptosis via two cell populations with distinctive cytological and molecular traits. Cell Growth Di ffer. 1998; 9:687–97.
22. Blagosklonny MV, Schulte T, Nguyen P, Trepel J, Neckers LM. Taxol-induced apoptosis and phosphorylation of Bcl-2 protein involves c-Raf-1 and represents a novel c-Raf-1 signal transduction pathway. Cancer Res. 1996; 56:1851–4. [PubMed: 8620503]
23. Oyaizu H, Adachi Y, Taketani S, Tokunaga R, Fukuhara S, Ikehara S. A crucial role of caspase 3 and caspase 8 in paclitaxel-induced apoptosis. Mol Cell Biol Res Commun. 1999; 2:36–41. [PubMed: 10527889]
24. Kataja V, Castiglione M. Locally recurrent or metastatic breast cancer: ESMO clinical recommendations for diagnosis, treatment and follow-up. Ann Oncol. 2008; 19(Suppl 2):ii11–3. [PubMed: 18456744]
25. Beslija S, Bonneterre J, Burstein HJ, Cocquyt V, Gnant M, Heinemann V, et al. Third consensus on medical treatment of metastatic breast cancer. Ann Oncol. 2009; 20:1771–85. [PubMed: 19608616]
26. National Comprehensive Cancer Network. [9 July 2009, date last accessed] NCCN Guidelines. 2009. http://www.nccn.org/professionals/physician_gls/f_guidelines.asp
27. DeNardo SJ, Kukis DL, Kroger LA, O'Donnell RT, Lamborn KR, Miers LA, et al. Synergy of Taxol and radioimmunotherapy with yttrium-90-labeled chimeric L6 antibody: efficacy and toxicity in breast cancer xenografts. Proc Natl Acad Sci U S A. 1997; 94:4000–4. [PubMed: 9108094]
28. O'Donnell RT, DeNardo SJ, Miers LA, Lamborn KR, Kukis DL, DeNardo GL, et al. Combined modality radioimmunotherapy for human prostate cancer xenografts with taxanes and 90 yttrium-DOTA-peptide-ChL6. Prostate. 2002; 50:27–37. [PubMed: 11757033]
29. Blumenthal RD, Leone E, Goldenberg DM. Tumor-specific dose scheduling of bimodal radioimmunotherapy and chemotherapy. Anticancer Res. 2003; 23:4613–9. [PubMed: 14981904]
30. Masters GR, Berger MA, Albone EF. Synergistic effects of combined therapy using paclitaxel and [90Y-DOTA]776. 1 on growth of OVCAR-3 ovarian carcinoma xenografts. Gynecol Oncol. 2006; 102:462–7. [PubMed: 16434088]
31. Kelly MP, Lee FT, Smyth FE, Brechbiel MW, Scott AM. Enhanced efficacy of 90Y-radiolabeled anti-Lewis Y humanized monoclonal antibody hu3S193 and paclitaxel combined-modality radioimmunotherapy in a breast cancer model. J Nucl Med. 2006; 47:716–25. [PubMed: 16595507]

32. Miers L, Lamborn K, Yuan A, Richman C, Natarajan A, DeNardo S, et al. Does paclitaxel (Taxol) given after (111)In-labeled monoclonal antibodies increase tumor-cumulated activity in epithelial cancers? Clin Cancer Res. 2005; 11:7158s–63s. [PubMed: 16203816]
33. Taghian AG, Abi-Raad R, Assaad SI, Casty A, Ancukiewicz M, Yeh E, et al. Paclitaxel decreases the interstitial fluid pressure and improves oxygenation in breast cancers in patients treated with neoadjuvant chemotherapy: clinical implications. J Clin Oncol. 2005; 23:1951–61. [PubMed: 15774788]
34. Folkman J. Tumor angiogenesis: therapeutic implications. N Engl J Med. 1971; 285:1182–6. [PubMed: 4938153]
35. Risau W. Mechanisms of angiogenesis. Nature. 1997; 386:671–4. [PubMed: 9109485]
36. Hicklin DJ, Ellis LM. Role of the vascular endothelial growth factor pathway in tumor growth and angiogenesis. J Clin Oncol. 2005; 23:1011–27. [PubMed: 15585754]
37. Kaku T, Kamura T, Kinukawa N, Kobayashi H, Sakai K, Tsuruchi N, et al. Angiogenesis in endometrial carcinoma. Cancer. 1997; 80:741–7. [PubMed: 9264358]
38. Kirschner CV, Alanis-Amezcua JM, Martin VG, Luna N, Morgan E, Yang JJ, et al. Angiogenesis factor in endometrial carcinoma: a new prognostic indicator? Am J Obstet Gynecol. 1996; 174:1879–82. discussion 82–4. [PubMed: 8678154]
39. Ferrara N, Gerber HP, LeCouter J. The biology of VEGF and its receptors. Nat Med. 2003; 9:669–76. [PubMed: 12778165]
40. Marty M, Pivot X. The potential of anti-vascular endothelial growth factor therapy in metastatic breast cancer: clinical experience with anti-angiogenic agents, focusing on bevacizumab. Eur J Cancer. 2008; 44:912–20. [PubMed: 18396037]
41. Presta LG, Chen H, O'Connor SJ, Chisholm V, Meng YG, Krummen L, et al. Humanization of an anti-vascular endothelial growth factor monoclonal antibody for the therapy of solid tumors and other disorders. Cancer Res. 1997; 57:4593–9. [PubMed: 9377574]
42. Willett CG, Boucher Y, di Tomaso E, Duda DG, Munn LL, Tong RT, et al. Direct evidence that the VEGF-specific antibody bevacizumab has antivascular effects in human rectal cancer. Nat Med. 2004; 10:145–7. [PubMed: 14745444]
43. Genentech, Inc. [11 March 2010, date last accessed] US Prescribing Information for Avastin. 2009. http://www.accessdata.fda.gov/drugsatfda_docs/label/2009/125085s0168lbl.pdf
44. F. Hoffmann-La Roche Ltd. [11 March 2010, date last accessed] Avastin Summary of Product Characteristics. 2009. http://www.emea.europa.eu/humandocs/PDFs/EPAR/avastin/emea-combinedh582en.pdf
45. Jain RK. Normalizing tumor vasculature with anti-angiogenic therapy: a new paradigm for combination therapy. Nat Med. 2001; 7:987–9. [PubMed: 11533692]
46. Ma J, Waxman DJ. Combination of antiangiogenesis with chemotherapy for more effective cancer treatment. Mol Cancer Ther. 2008; 7:3670–84. [PubMed: 19074844]
47. Ansiaux R, Baudelet C, Jordan BF, Beghein N, Sonveaux P, De Wever J, et al. Thalidomide radiosensitizes tumors through early changes in the tumor microenvironment. Clin Cancer Res. 2005; 11:743–50. [PubMed: 15701864]
48. Dings RP, Loren M, Heun H, McNiel E, Griffioen AW, Mayo KH, et al. Scheduling of radiation with angiogenesis inhibitors anginex and Avastin improves therapeutic outcome via vessel normalization. Clin Cancer Res. 2007; 13:3395–402. [PubMed: 17545548]
49. Salaun PY, Bodet-Milin C, Frampas E, Oudoux A, Sai-Maurel C, Faivre-Chauvet A, et al. Toxicity and efficacy of combined radioimmunotherapy and bevacizumab in a mouse model of medullary thyroid carcinoma. Cancer. 2010; 116:1053–8. [PubMed: 20127950]
50. Chan A, Miles DW, Pivot X. Bevacizumab in combination with taxanes for the first-line treatment of metastatic breast cancer. Ann Oncol. 2010; 21:2305–15. [PubMed: 20335367]
51. Pastan I, Lovelace ET, Gallo MG, Rutherford AV, Magnani JL, Willingham MC. Characterization of monoclonal antibodies B1 and B3 that react with mucinous adenocarcinomas. Cancer Res. 1991; 51:3781–7. [PubMed: 1648444]
52. Camera L, Kinuya S, Garmestani K, Brechbiel MW, Wu C, Pai LH, et al. Comparative biodistribution of indium- and yttrium-labeled B3 monoclonal antibody conjugated to either 2-(p-

SCN-Bz)-6-methyl-DTPA (1B4M-DTPA) or 2-(p-SCN-Bz)-1,4,7,10-tetraazacyclododecane tetraacetic acid (2B-DOTA). Eur J Nucl Med. 1994; 21:640–6. [PubMed: 7957350]

53. Camera L, Kinuya S, Garmestani K, Pai LH, Brechbiel MW, Gansow OA, et al. Evaluation of a new DTPA-derivative chelator: comparative biodistribution and imaging studies of 111In-labeled B3 monoclonal antibody in athymic mice bearing human epidermoid carcinoma xenografts. Nucl Med Biol. 1993; 20:955–62. [PubMed: 8298575]
54. Yao Z, Zhang M, Axworthy DB, Wong KJ, Garmestani K, Park L, et al. Radioimmunotherapy of A431 xenografted mice with pretargeted B3 antibody-streptavidin and (90)Y-labeled 1,4,7,10-tetraazacyclododecane-N,N′,N″,N‴-tetraacetic acid (DOTA)-biotin. Cancer Res. 2002; 62:5755–60. [PubMed: 12384535]
55. Dreher MR, Liu WG, Michelich CR, Dewhirst MW, Yuan F, Chilkoti A. Tumor vascular permeability, accumulation, and penetration of macromolecular drug carriers. J Natl Cancer I. 2006; 98:335–44.
56. Bozec A, Sudaka A, Fischel JL, Brunstein MC, Etienne-Grimaldi MC, Milano G. Combined effects of bevacizumab with erlotinib and irradiation: a preclinical study on a head and neck cancer orthotopic model. Br J Cancer. 2008; 99:93–9. [PubMed: 18577994]
57. Zhang Y, Xiang L, Hassan R, Paik CH, Carrasquillo JA, Jang BS, et al. Synergistic antitumor activity of taxol and immunotoxin SS1P in tumor-bearing mice. Clin Cancer Res. 2006; 12:4695–701. [PubMed: 16899620]
58. Holden SA, Lan Y, Pardo AM, Wesolowski JS, Gillies SD. Augmentation of antitumor activity of an antibody-interleukin 2 immunocytokine with chemotherapeutic agents. Clin Cancer Res. 2001; 7:2862–9. [PubMed: 11555604]
59. Wen PY, Macdonald DR, Reardon DA, Cloughesy TF, Sorensen AG, Galanis E, et al. Updated response assessment criteria for high-grade gliomas: response assessment in neuro-oncology working group. J Clin Oncol. 2010; 28:1963–72. [PubMed: 20231676]
60. Varallyay CG, Muldoon LL, Gahramanov S, Wu YJ, Goodman JA, Li X, et al. Dynamic MRI using iron oxide nanoparticles to assess early vascular effects of antiangiogenic versus corticosteroid treatment in a glioma model. J Cerebr Blood F Met. 2009; 29:853–60.
61. Griffon-Etienne G, Boucher Y, Brekken C, Suit HD, Jain RK. Taxane-induced apoptosis decompresses blood vessels and lowers interstitial fluid pressure in solid tumors: clinical implications. Cancer Res. 1999; 59:3776–82. [PubMed: 10446995]
62. Winkler F, Kozin SV, Tong RT, Chae SS, Booth MF, Garkavtsev I, et al. Kinetics of vascular normalization by VEGFR2 blockade governs brain tumor response to radiation: role of oxygenation, angiopoietin-1, and matrix metalloproteinases. Cancer Cell. 2004; 6:553–63. [PubMed: 15607960]
63. Wachsberger P, Burd R, Dicker AP. Tumor response to ionizing radiation combined with antiangiogenesis or vascular targeting agents: exploring mechanisms of interaction. Clin Cancer Res. 2003; 9:1957–71. [PubMed: 12796357]
64. Kim YC, Kim YH, Uhm SH, Seo YS, Park EK, Oh SY, et al. Radiation Safety Issues in Y-90 Microsphere Selective Hepatic Radioembolization Therapy: Possible Radiation Exposure from the Patients. Nuclear Medicine and Molecular Imaging. 2010; 44:252–60.
65. Koppe MJ, Bleichrodt RP, Soede AC, Verhofstad AA, Goldenberg DM, Oyen WJ, et al. Biodistribution and therapeutic efficacy of (125/131)I-, (186)Re-, (88/90)Y-, or (177)Lu-labeled monoclonal antibody MN-14 to carcinoembryonic antigen in mice with small peritoneal metastases of colorectal origin. J Nucl Med. 2004; 45:1224–32. [PubMed: 15235070]
66. Sugahara KN, Teesalu T, Karmali PP, Kotamraju VR, Agemy L, Greenwald DR, et al. Coadministration of a tumor-penetrating peptide enhances the efficacy of cancer drugs. Science. 2010; 328:1031–5. [PubMed: 20378772]

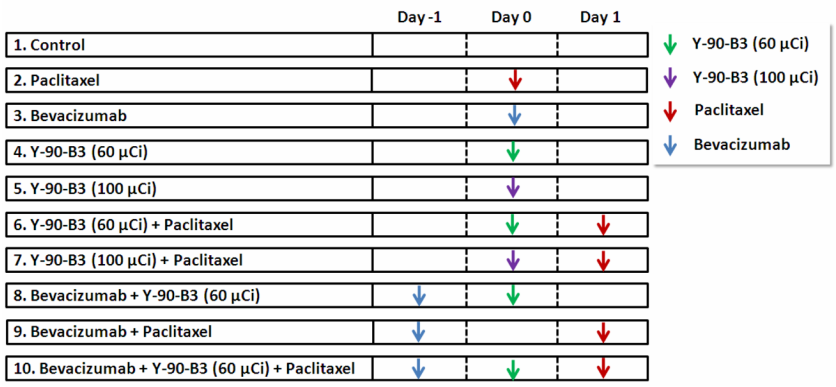


**Fig. 1.**

Drug treatment time line.

Groups of nude mice (n = 4–9 mice/group) were inoculated *s.c.* with A431 tumor cells expressing the $Le^y$ antigen on the right hind flank. When the tumor size was approximately 200 $mm^3$, the mice received a single dose of *i.v.* $^{90}$Y-labeled B3 (60 μCi/150 μg or 100 μCi/150 μg B3), *i.p.* Paclitaxel (40 mg/kg), or *i.v.* Bevacizumab (5 mg/kg) for a monotherapy. For a combined radioimmunotherapy with Paclitaxel or Bevacizumab, the mice received $^{90}$Y-B3 and Paclitaxel (40 mg/kg) or Bevacizumab (5 mg/kg) and $^{90}$Y-B3 at 1-day interval. For a combined therapy of Bevacizumab with Paclitaxel, the mice received Bevacizumab and Paclitaxel at 2-day interval. For a combined therapy with three agents, the mice were treated with Bevacizumab, $^{90}$Y -B3 (60 μCi/150 μg) and Paclitaxel each at 1 day intervals. The mice with no treatment were used as a control.

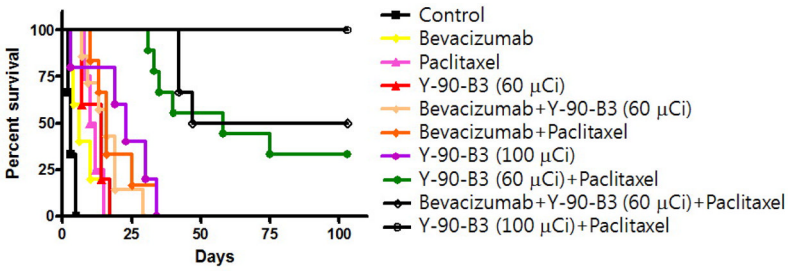


**Fig. 2.**

Kaplan-Meier survival plot for the combination therapies.

The tumor volume was plotted over time for each mouse and the day at which tumor volume passed 1,000 $mm^3$ was used as a surrogate endpoint of survival. The Kaplan-Meir plot was performed using GraphPad Prism 5 (GraphPad Software, La Jolla, CA).

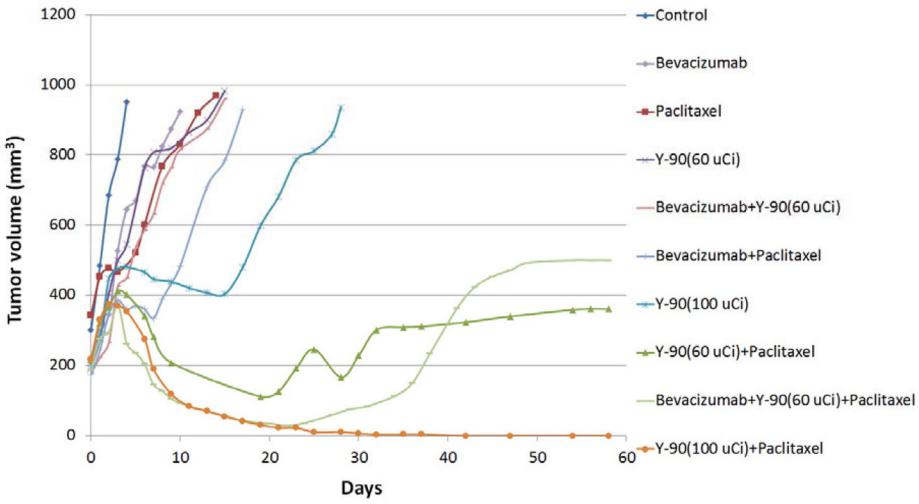


**Fig. 3.**

Effect of different treatment regimes on Tumor growth. Groups of nude mice (n = 4–9 mice/group) implanted *s.c.* with A431 tumor were treated as described in Fig. 1. The tumor volume was measured from each mouse. The mean tumor volume was calculated at each time point and plotted over time to construct a mean tumor growth curve. The combined therapy involving $^{90}$Y-B3 treatment followed by Paclitaxel treatment produced a remarkable synergistic effect on tumor shrinkage and an increase in median survival time: 3 of 9 mice (33%) and 6 of 6 mice (100%) were alive with no tumor ($P < 0.001$) on day 120 when treated with a combined therapy involving 60 μCi $^{90}$Y-B3 or 100 μCi $^{90}$Y-B3 and Paclitaxel, respectively. The addition of Bevacizumab treatment to the combined therapy of 60 μCi $^{90}$Y-B3 and Paclitaxel provided an additive effect in survival with 3 of 6 (50%) alive with no tumor compared to a survival rate of 33% for the combined therapy of 60 μCi $^{90}$Y-B3 and Paclitaxel. However, this Bevacizumab effect was statistically insignificant ($P > 0.05$). The tumor volumes of all other treatment groups passed the surrogate endpoint (1000 $mm^3$) by day 35.

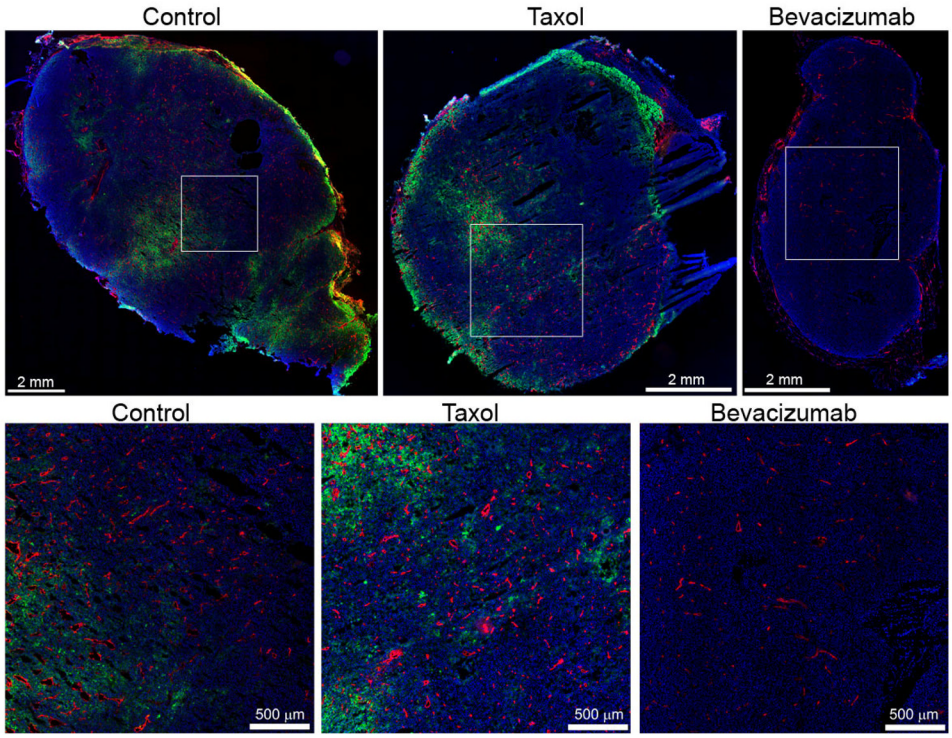


**Fig. 4.**

Summary of antibody distribution. B3 antibody (green), blood vessels (red), and nuclei (blue) are shown for each group as a whole tumor (top row) and with higher magnification (bottom row) to better appreciate the vascular density and antibody distribution. The B3 antibody channel was acquired and displayed with consistent levels, while the blood vessels and nuclei are displayed to maximize contrast.

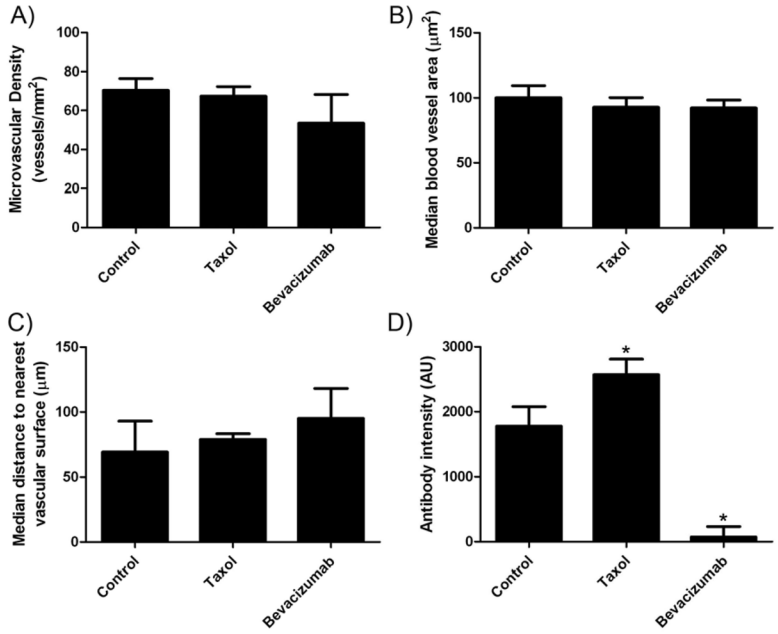


**Fig. 5.**

Summary of vascular parameters and antibody delivery. A) Microvascular density (MVD) of A431 tumors following treatment with Paclitaxel or Bevacizumab. B) Median blood vessel area of A431 tumors following treatment with Paclitaxel or Bevacizumab. C) The median distance of a tumor pixel to the nearest blood vessel surface (vascular architecture). D) Antibody accumulation in tumor sections determined by epi-fluorescent microscopy overall intensity. Data are mean (A and D) or median (B and C) ± SEM shown as error bars unless otherwise indicated (n = 4–5). * Indicates P-value < 0.05 versus control.

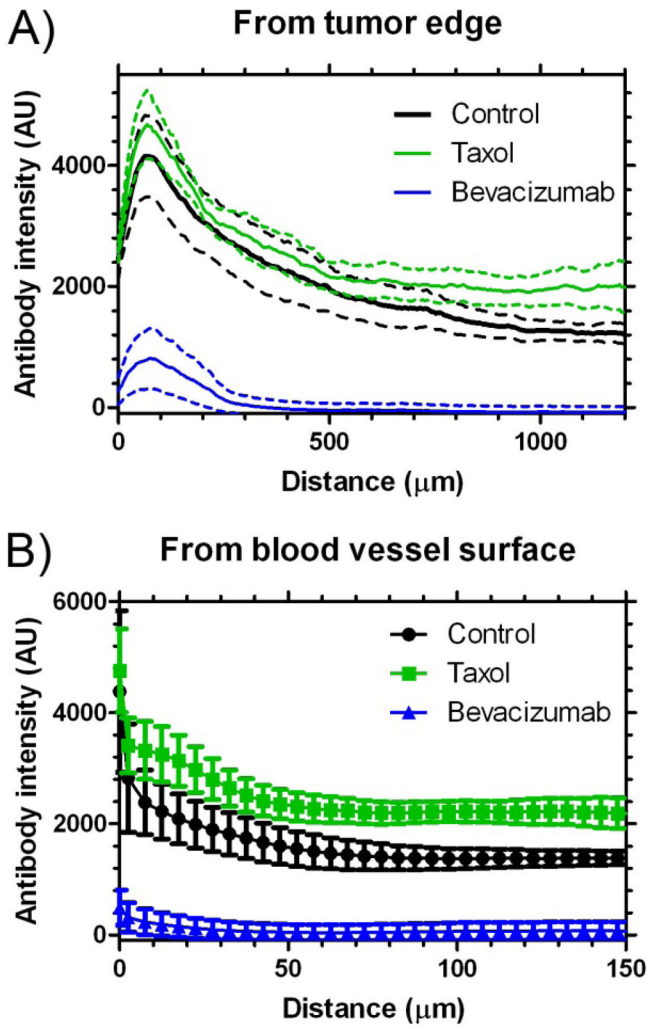


**Fig. 6.**

Antibody penetration from the tumor edge (A) or blood vessel surface (B). Data are mean ± SEM. Mean is shown as a solid line and SEM as a dashed line (A) or error bars (B), n = 4–5. Paclitaxel and Bevacizumab treated groups are significantly different from the control group (P-value < 0.05).

**Table 1**

Effect of Paclitaxel and Bevacizumab on median survival time when combined with $^{90}$Y-B3

| | Group | Total Number of Animal | Median Survival Day[a)] | Tumor Response[b)] | | | Survival (%) |
|---|---|---|---|---|---|---|---|
| | | | | NR(%) | PR(%) | C(%) | |
| 1 | Control | 4 | 4 | 4(100) | | | 0 (0) |
| 2 | Paclitaxel | 4 | 11 | 4 (100) | | | 0 (0) |
| 3 | Bevacizumab | 5 | 6 | 5 (100) | | | 0 (0) |
| 4 | Y-90-B3 (60 μCi) | 5 | 14 | 5 (100) | | | 0 (0) |
| 5 | Y-90-B3 (100 μCi) | 5 | 23 | 4 (100) | | | 0 (0) |
| 6 | Y-90-B3 (60 μCi)+ Paclitaxel | 9 | 58 | 5(56) | 1 (11) | 3 (33) | 3 (33) |
| 7 | Y-90-B3(100 μCi)+ Paclitaxel | 6 | Undefined | | | 6(100) | 6 (100) |
| 8 | Bevacizumab +Y-90-B3 (60 μCi) | 6 | 16 | 6(100) | | | 0(0) |
| 9 | Bevacizumab + Paclitaxel | 6 | 16 | 6(100) | | | 0(0) |
| 10 | Bevacizumab + Y-90-B3 (60 μCi) + Paclitaxel | 6 | 75 | 3(50) | | 3 (50) | 3 (50) |

[a)] Median survival day was calculated by GraphPad Prism 4 (GraphPad Software, Inc.).

[b)] Tumor responses were categorized as follows: C, complete cure (Tumor disappeared and did not regrow by the end of the 120-day study); PR, partial response (The tumor volume decreased by 50% or more for at least 7 days and then regrew); NR, no response.